Neuron, Vol. 20, 773–781, April, 1998, Copyright ©1998 by Cell Press

Visualization of Cyclic AMP–Regulated Presynaptic Activity at Cerebellar Granule Cells

Pascale Chavis,* Patrice Mollard,† Joël Bockaert,* and Olivier Manzoni*‡
*Centre National pour la Recherche Scientifique
†Institut National de la Sante et de la Recherche Medicale
141, Rue de la Cardonille
34094 Montpellier Cedex 05
France

Summary

Adenylyl cyclase (AC) modulation of vesicular cycling was visualized at cultured cerebellar granule cell synapses using the sequential uptake of antibodies directed against the intraluminal domain of synaptotagmin I. Vesicle recycling due to spontaneous transmitter release in the absence of action potentials was increased by the AC/protein kinase A (PKA) activators forskolin and CPT–cAMP. These effects were blocked by the PKA inhibitor Rp–cAMPs. Cyclic AMP elevation also induced new cycling at previously silent sites. Activation of L-AP4–sensitive mGluR reduced the cAMP/PKA enhancement at preexisting synapses downstream of both AC and calcium channels. Modulation of the turnover and the number of vesicular release sites provide one mechanism that may underlie cAMP-dependent cerebellar long-term potentiation.

Introduction

Studies of activity-dependent enhancement of synaptic strength at hippocampal excitatory synapses have revealed two distinct types of long-term potentiation (LTP), the classical N-methyl-D-aspartate (NMDA) receptor–dependent LTP of CA1 pyramidal cells and an NMDA receptor–independent LTP at hippocampal mossy fiber–CA3 synapses. The latter form is dependent on the presynaptic activation of adenylyl cyclase (AC) (Zalutsky and Nicoll, 1990; Huang et al., 1994; Weisskopf et al., 1994). A similar form of cAMP-dependent enhancement has recently been described at the cerebellar parallel fiber terminals (Salin et al., 1996; Chen and Regher, 1997). Granule cells of the cerebellum also express mGluR4 metabotropic glutamate receptors that are known to inhibit both cAMP accumulation (Conn and Pin, 1997) and transmitter release at many synapses (Tanabe et al., 1993; Saugstad et al., 1994; Ohishi et al., 1995). Interestingly, at the parallel fiber synapse mGluR4 receptors have been shown to be exclusively located at presynaptic terminals (Kinoshita et al., 1996). Recent mGluR4 knockout experiments (Pekhletski et al., 1996) have suggested a role for this receptor in controlling the availability of glutamate vesicles in the cerebellum. Thus, the interplay between the cAMP/protein kinase A (PKA) cascade and mGluR4 might directly control presynaptic vesicular release at the parallel fiber synapse.

Many studies have examined activity-dependent synaptic plasticity by recording from populations of synapses reflecting the average changes in properties of many individual release sites. However, release sites display significant heterogeneity in their presynaptic properties (Rosenmund et al., 1993; Malgaroli et al., 1995; Dobrunz and Stevens, 1997; Murthy et al., 1997). Moreover, the ability to induce facilitation/LTP seems to be inversely correlated to the initial release probability of the presynaptic neuron (Malgaroli et al., 1995; Dobrunz and Stevens, 1997; Murthy et al., 1997). The physiological basis for this apparent presynaptic heterogeneity is still unknown.

We used a new noninvasive technique to directly visualize exocytotic–endocytotic cycling at single presynaptic terminals of cerebellar granule cells to explore the mechanisms that may underlie cAMP-dependent LTP of cerebellar parallel fibers. This assay is based on the sequential uptake of antibodies targeted against the luminal epitope of the vesicular protein synaptotagmin I (Matteoli et al., 1992; Elferink et al., 1993; Elferink and Scheller, 1995). Imaging of anti–synaptotagmin I immunoreactivity uptake provides a direct presynaptic quantitation of synaptic release, does not require measurements of postsynaptic signals (Malgaroli et al., 1995), and has the key advantage over the FM1–43 technique (Betz and Bewick, 1992; Ryan et al., 1996) of allowing the detection of release sites that are inactive (i.e., "silent") during the control period.

Here, we provide evidence that the cAMP/PKA cascade augments vesicular release at cerebellar granule cell synapses in primary culture. Activation of L-2-amino-4-phosphonobutyrate (L-AP4) -sensitive mGluRs completely blocked the cAMP/PKA enhancement downstream of both AC- and voltage-dependent Ca^{2+} channels and only at the presynaptic terminal, consistent with a restricted presynaptic localization for these mGluRs. At individual release sites, there was an inverse relationship between the amount of cAMP/PKA potentiation and the initial vesicular activity. Activation of the cAMP/PKA cascade also induced anti–synaptotagmin I uptake at sites that were inactive during the control period, suggesting the existence of "silent" release sites.

Results

Presynaptic Localization of Anti-Synaptotagmin Antibodies

When cerebellar granule synapses in culture were fixed and permeabilized, a clear colocalization of the rabbit anti-synaptophysin (red, Figure 1A) with anti–synaptotagmin I staining (green, Figure 1B) was found. Figure 1C shows the superimposition of synaptotagmin and synaptophysin staining, indicating a specific presynaptic localization of synaptotagmin I immunoreactivity. Figure 1D shows the distribution of rabbit and goat anti-synaptotagmin immunoreactivity in β-tubulin–positive

‡To whom correspondence should be addressed. Present address: Vollum Institute, Oregon Health Sciences University L-474, 3181 S.W. Sam Jackson Park Road, Portland, Oregon 97201.

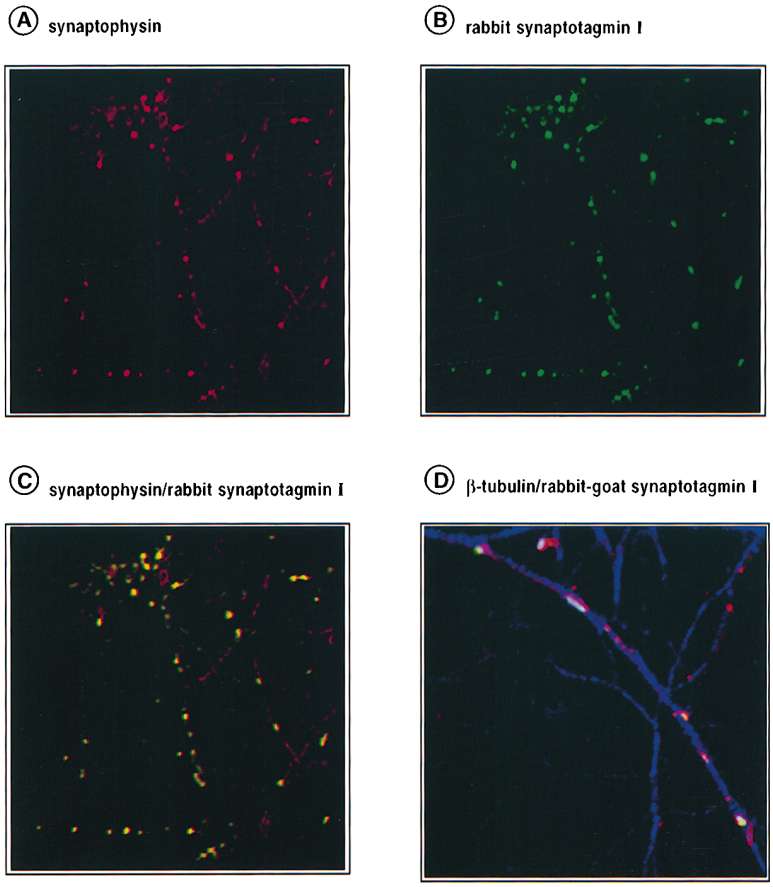

Figure 1. Anti–Synaptotagmin I Antibodies Specifically Label Synaptic Sites on Cultured Cerebellar Granule Cells

Specific synaptic localization of antibodies to synaptotagmin I.

(A–C) Confocal microscopy imaging of staining performed on fixed and permeabilized cells: (A) anti-synaptophysin (red), (B) rabbit anti-synaptotagmin (green), and (C) superimposition of images (A) and (B).

(D) Confocal microscopy imaging of staining performed on fixed and permeabilized cells: β-tubulin (blue) + rabbit anti-synaptotagmin (green) + goat anti-synaptotagmin (red). Superimposition of rabbit anti-synaptotagmin and goat anti-synaptotagmin labeling gives the bright yellow spots.

granule cell processes (blue). Together, these data demonstrated that both goat and rabbit anti–synaptotagmin I antibodies only targeted synaptic vesicles in granule neurons. In all subsequent experiments, all synaptotagmin immunoreactive sites were considered to be synaptic specializations and were included in the analyses (see below).

Dynamic Uptake of Anti-Synaptotagmin Antibodies

All experiments were performed in the presence of tetrodotoxin, so that the vesicular cycling being measured was due to spontaneous fusion and recovery of vesicles in the absence of action potentials firing. To visualize spontaneous vesicular cycling at individual active cerebellar granule cell synapses, cerebellar granule neurons were sequentially incubated with goat anti–synaptotagmin I for 1 hr (first period of staining: 1 hr, P1) and with rabbit anti–synaptotagmin I (second period of staining: 1 hr, P2). Using a confocal microscope system, the amount of anti–synaptotagmin I internalized during periods P1 and P2 was quantified. The boundaries of the regions of interest were demarcated for the first image (goat anti-synaptotagmin, fluorescence F1), and fluorescent intensity was quantified over the pixels within the same region for the second subsequent image (rabbit anti-synaptotagmin, fluorescence F2). All fluorescent spots were included in the analysis; that is, there was no selection of the analyzed boutons. The ratio of intensity F2/F1 gave a measure of vesicular cycling, as originally described by Malgaroli et al. (1995).

cAMP Stimulates Vesicular Cycling

Since electrophysiological experiments using the cerebellar slice preparation have shown a presynaptic cAMP-dependent LTP at the parallel fiber synapses (Salin et al., 1996), the effects of intracellular cAMP levels on vesicular cycling were first investigated.

In control, both the pattern and relative amount of anti–synaptotagmin I fluorescence remained stable (F2/F1 = 0.370 ± 0.013, n = 490 synapses; Figure 2A). Application of the membrane-permeant AC activator forskolin (FSK, 10 μM) (Seamon and Daly, 1986) for 1 hr during P2 (a protocol referred as FSK 1h) increased by 5-fold the spontaneous vesicular cycling at cerebellar granule cell synapses. The F2/F1 ratio calculated was 1.824 ± 0.09 (n = 407 synapses) in FSK-stimulated neurons ($p < 0.0001$, t test) compared to 0.370 ± 0.013 (n = 490 synapses) in control (Figure 2D). Similar results were obtained regardless of the order of incubation with goat and rabbit antibodies (data not shown). The inactive analog of FSK, dideoxy-FSK (10 μM, 1 hr), was without effect (F2/F1 = 0.368 ± 0.032, n = 184 synapses), suggesting that the FSK enhancement was due to activation of AC.

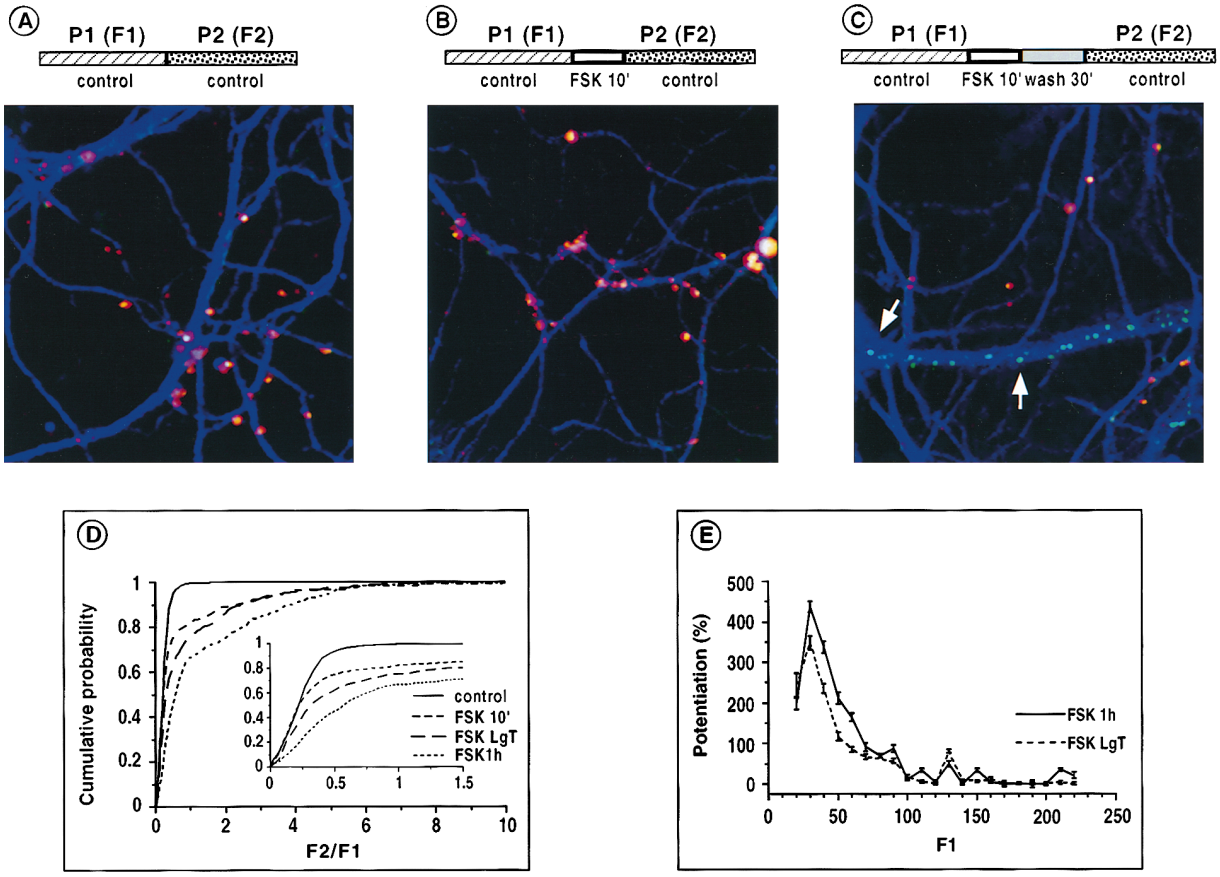

Figure 2. Forskolin Activates Vesicular Cycling in Cerebellar Cultures

(A–C) Superimposed images of synaptotagmin I and β-tubulin labelings. The release activity of individual cerebellar synapses was visualized by confocal microscopy analysis of the sequential exposure of cerebellar granule cells to goat (red fluorescence, P1) and rabbit (green fluorescence, P2) anti–synaptotagmin I antibodies. The blue fluorescence corresponds to the β-tubulin labeling. When superimposed, red F1 fluorescence and green F2 fluorescence gave a yellow labeling. The boundaries of all of the Texas red–stained boutons were demarcated for the first image (control period, F1), and fluorescent intensity was quantitated over the pixels within the corresponding fluorescein-stained region on the subsequent image (stimulated period, F2). (A) shows dynamic uptake of anti–synaptotagmin I antibodies in control conditions. The exocytotic activity measured during the period P2 was enhanced by either a 10 min application of FSK between P1 and P2 (B) or a 10 min FSK application followed by a 30 min wash (C). Note the appearance of new release sites (arrows, green spots) silent during P1, preferentially localized on the soma or between the soma and the first branching (C). The large bright spots occurred when fluorescence from several single release sites overlapped (B).

(D) Cumulative probability distributions of F2/F1 values for individual synapses in control conditions (cont), during a 1 hr application of FSK (FSK 1h), after a 10 min FSK application (FSK 10′), and during the long-term paradigm (10 min FSK application followed by a 30 min wash, FSK LgT). The inset shows a scale enlargement of the cumulative probability histogram.

(E) Correlation of the basal level of synaptic activity with the enhancement of vesicular cycling induced by either a 1 hr FSK application (FSK 1h) or a 10 min FSK application followed by a 30 min wash (FSK LgT). Mean percentage of potentiation was calculated according to the following formula: $\{[(F2/F1)FSK/(F2/F1)cont] - 1\} \times 100$, for subgroups of synapses binned according to their F1 values. Bars indicated SEM and were derived from the formula: $variance = variance_{FSK} + variance_{cont}$.

We next asked if brief stimulation of cAMP with FSK was accompanied by a long-lasting enhancement of vesicular release. Forskolin applied for 10 min between P1 and P2 (a protocol intended to mimic protocols used to induce LTP in slices and referred as FSK 10′ [Salin et al., 1996]) caused an enhancement of vesicular cycling by >2-fold (F2/F1 = 0.852 ± 0.068, n = 558 synapses, p = 0.001, t test; Figures 2B and 2D). The enhanced F2/F1 ratio lasted for at least 1.5 hr after washing the FSK (a protocol referred as FSK LgT). In this condition, there still was an increase of vesicular cycling by >2-fold (0.993 ± 0.079, n = 635 synapses, p = 0.0003, t test; Figure 2C). These experiments are summarized in Figure 2D (see Experimental Procedures).

Does the amplitude of the cAMP enhancement at a given synapse depend on previous exocytotic activity? There was a strong positive correlation between F1 and F2 in control conditions (slope = 0.89, r = 0.77, n = 490, p < 0.001), indicating that unstimulated synapses (i.e., in the absence of FSK) had similar levels of activity during P1 and P2. To examine if the degree of potentiation at individual synapses was correlated with previous synaptic activity before potentiation, individual synapses were classified according to their F1 values, and then

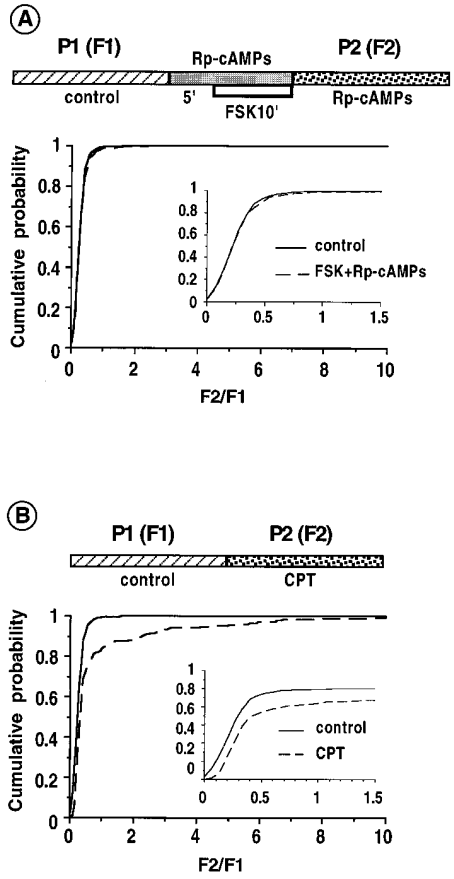

Figure 3. A Role for the cAMP/PKA Cascade in the Enhancement of Vesicular Recycling

(A) Effect of Rp–cAMPs on the 10 min FSK-evoked stimulation of presynaptic activity. Cumulative probability distributions are of F2/F1 values for synapses in control conditions and when Rp–cAMPs treatment started 5 min before the application of FSK (10 min) and ended 1 hr after.

(B) Cumulative probability distributions of F2/F1 values for individual synapses showing that a 1 hr application of the cAMP analog CPT–cAMP (CPT) enhanced synaptic vesicular cycling.

the mean percentage of potentiation for each class was calculated. The highest degree of potentiation was achieved by synapses that had an initially lower F1 value (<70 fluorescent arbitrary units), whereas synapses with the highest initial exocytotic activity showed no cAMP-dependent potentiation (Figure 2E).

Coincubating the granule cells with a membrane-permeant blocker of the regulatory site of PKA, Rp-adenosine-3′,5′-cyclic monophosphothioate triethylamine (Rp–cAMPs, 500 μM), completely prevented the FSK-induced enhancement of vesicular release (Figure 3A). In the presence of Rp–cAMPs and FSK, F2/F1 remained at its basal value (F2/F1 = 0.324 ± 0.01, n = 498 synapses, p = 0.932, t test, when compared to control). Likewise, the membrane-permeant cAMP analog 8-(4-chlorophenylthio)-adenosine-3′-5′monophosphate cyclic AMP (CPT–cAMP, 500 μM, 1 hr; Figure 3B) produced a 3-fold increase in vesicular cycling (F2/F1 = 0.928 ± 0.092, n = 376 synapses, p = 0.004, t test). Thus, the increased vesicular turnover appears to be dependent on the activation of PKA.

cAMP Induces New Vesicular Cycling at Previously Inactive Uptake Sites

The study of presynaptic cAMP-dependent LTP in autaptic cultures of hippocampal granule cells has led to the proposal that this form of plasticity is accompanied by a "switching on" of silent release sites (Tong et al., 1996). We checked for the presence of silent synapses in our model.

In each of the experiments described above, FSK induced anti–synaptotagmin I uptake at sites that were previously inactive during the control incubation period. An example is given in Figure 2C, where arrows show new anti–synaptotagmin I uptake sites unmasked by application of FSK (10 min FSK followed by 30 min wash, green spots). On average, "the long-term FSK" treatment led to a 1.77- ± 0.17-fold increase in the number of active uptake sites (n = 10 independent experiments, 360 synapses). New release sites were visualized after the 1 hr and the 10 min FSK treatment, which both gave similar increases in the number of new release sites (1.73- ± 0.15-fold and 1.70- ± 0.08-fold increase in the number of release sites, p = 0.885, n = 8 and 6 experiments and n = 367 and 349 synapses, respectively). Interestingly, 61.5% ± 8.5% of the new release sites appeared between the soma and the first branching of the neurite, whereas 28.1% ± 7.9% were found directly on the soma (Table 1). CPT–cAMP (500 μM) induced the appearance of new uptake sites, although to a much lesser extent than FSK (1.19- ± 0.08-fold increase, n = 9 experiments and n = 340 synapses, p = 0.006 when compared to FSK).

L-AP4–Sensitive mGluRs Modulate Basal and cAMP-Induced Release Downstream of the Adenylyl Cyclase

It was interesting to determine if receptor-mediated regulation of AC would alter the cAMP dependence of vesicular release. L-AP4–sensitive mGluRs are coupled to the inhibition of the cyclase, and in situ hybridization studies have revealed the highest levels of mGluR4 mRNA in the granule cells of the cerebellum (Prézeau et al., 1994; Saugstad et al., 1994; Ohishi et al., 1995). We next evaluated whether glutamate presynaptic autoreceptors sensitive to the synthetic glutamate analog L-AP4 (Cotman et al., 1986; Mayer and Westbrook, 1987) could regulate vesicular cycling.

The effects of L-AP4 on the FSK enhancement of vesicular cycling were measured. The presence of 20 μM L-AP4 completely blocked the FSK 1h enhancement of vesicular cycling (F2/F1 = 0.242 ± 0.02, n = 148 synapses, p < 0.0001, t test, when compared to the control FSK 1h effect). Similar results were obtained when the effects of 20 μM L-AP4 were tested on the enhancement induced by shorter periods of FSK (10 min; Figures 4A and 4B) (F2/F1 = 0.286 ± 0.021, n = 253 synapses, p = 0.0003, t test, when compared to the control 10 min FSK effect). L-AP4 at both concentrations of 20 μM and 200 μM decreased basal vesicular cycling (i.e., in the absence of stimulated-cAMP accumulation, F2/F1 = 0.279 ± 0.016, n = 120 synapses, p = 0.003, t test; Figure 4C). The relatively high affinity of L-AP4, the high level of mGluR4 mRNA in the cerebellum, and the present results are consistent with inhibition of vesicular release by mGluR4 receptors.

Table 1. cAMP Elevation Activates Silent Release Sites

Treatment		FSK 1h	FSK 10′	FSK Long-Term	CPT 1h
Localization	soma (%)	nd	28.1 ± 7.9 n = 77	21.7 ± 9.6 n = 168	24.9 ± 6.6 n = 52
	soma → first branching (%)	76.4 ± 18.9 n = 61	61.5 ± 8.5 n = 77	62.6 ± 8.7 n = 168	63.5 ± 11.1 n = 52

n is the total number of new release sites.
nd, not determined.

When vesicular cycling was stimulated with the cAMP analog CPT–cAMP (500 μM, 1 hr, P2 period) to bypass the AC-dependent step, we still observed clear inhibitory actions of L-AP4 (20 μM, F2/F1 = 0.225 ± 0.01, n = 293 synapses, $p < 0.001$, t test, when compared to CPT–cAMP alone; Figure 4D). This suggests that mGluR4-mediated depression of both basal and stimulated vesicular release is not due to a decrease of intracellular cAMP levels but rather to the modulation of processes downstream of the AC stimulation.

Strikingly, the inhibition by L-AP4 was restricted to preexisting release sites (mainly located close to or at the synaptic terminals). L-AP4 incubation had little or no effect on the amount or the localization of new anti–synaptotagmin I uptake sites evoked by cAMP (Figure 4A, arrows). When applied in the presence of L-AP4, FSK still induced the appearance of new release sites. Indeed, FSK caused a 1.68- ± 0.16-fold increase in the number of release sites in the presence of L-AP4, compared to 1.70 ± 0.08 when FSK was applied alone ($p = 0.786$, n = 11 and 6 individual experiments, respectively; Table 2). Similar results were obtained when cells were treated with CPT–cAMP in the presence of L-AP4. There was a 1.18- ± 0.1-fold increase in the number of release sites for CPT–cAMP + L-AP4 compared to 1.19 ± 0.08 for CPT–cAMP alone ($p = 0.927$, n = 5 and 9 individual experiments, respectively; Table 2).

mGluR4 and cAMP Regulate Vesicular Cycling Downstream of Calcium Channels

Two presynaptic mechanisms for the modulation of transmitter release are classically described: (1) direct interference with the systems responsible for the Ca^{2+} influx in the synaptic terminal or (2) direct modulation of the vesicular machinery ("downstream of the Ca^{2+} influx") (Wu and Saggau, 1997).

The actions of FSK and of CPT–cAMP were insensitive to the Ca^{2+} channel blocker Cd^{2+} (100 μM) (Figure 5A; for FSK + Cd^{2+}: F2/F1 = 0.981 ± 0.092, n = 271, $p = 0.928$, t test, when compared to FSK alone; for CPT–cAMP + Cd^{2+}: F2/F1 = 0.959 ± 0.17, n = 242, $p = 0.786$, t test, when compared to CPT–cAMP alone).

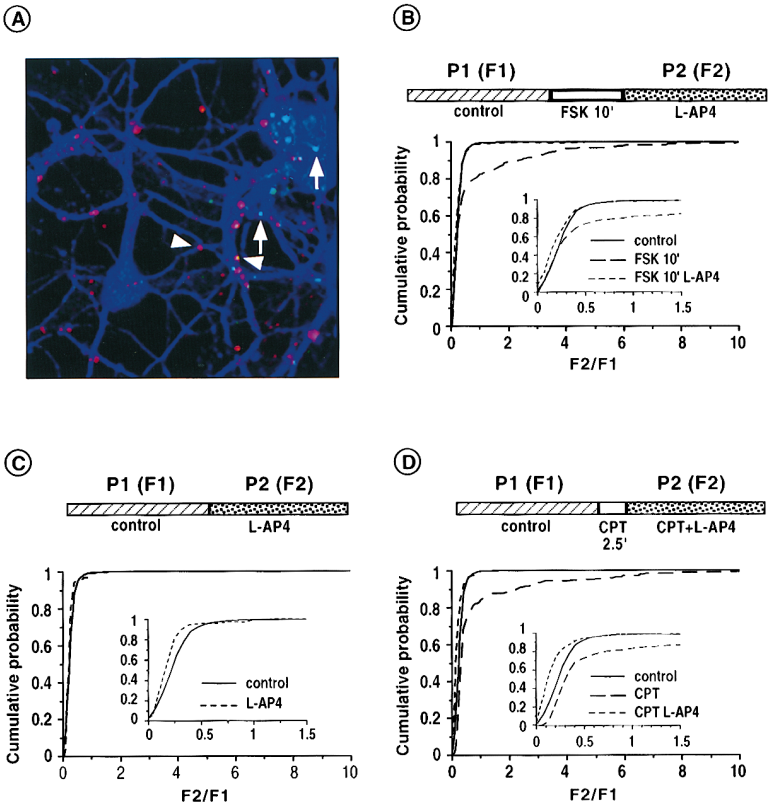

Figure 4. Modulation of Basal and cAMP/PKA–Enhanced Vesicular Release by L-AP4–Sensitive Glutamate Autoreceptors

(A) Confocal imaging of anti–synaptotagmin I labeling during L-AP4 inhibition of the FSK enhancement. L-AP4 treatment did not affect the "switch on" of silent release sites (arrows, green labeling), but it decreased the cAMP enhancement at existing release sites (arrowheads).

(B–D) Cumulative probability distributions of F2/F1 values for individual synapses showing the blocking effect of L-AP4 on (B) the FSK-mediated enhancement of recycling (FSK 10′ L-AP4), (C) the basal synaptic recycling (L-AP4), and (D) the CPT-induced enhancement of vesicular cycling (CPT L-AP4).

Table 2. Lack of Effect of L-AP4 on Silent Release Sites Activated by cAMP

Treatment		FSK 10′ + L-AP4	CPT 1h + L-AP4
Localization	soma (%)	27.5 ± 8.8 n = 48	nd
	soma → first branching (%)	65.2 ± 9.6 n = 48	65.9 ± 13.6 n = 34

n is the total number of new release sites.
nd, not determined.

These results exclude "an upregulation of presynaptic voltage-dependent Ca^{2+} channels" as a cause of the cAMP enhancement of vesicular activity (Salin et al., 1996) and support the notion that the action is downstream of the Ca^{2+} channels (Chen and Regher, 1997). Electrophysiological experiments have shown that neurotransmitters such as adenosine, GABA, and glutamate modulate presynaptic release both at the level of the Ca^{2+} channel and downstream of the Ca^{2+} entry (Wu and Saggau, 1994, 1995, 1997; Tyler and Lovinger, 1995; Scanziani et al., 1995). The inhibition of vesicular recycling by L-AP4–sensitive mGluRs was also insensitive to prior treatment with Cd^{2+} (Figure 5B; F2/F1 = 0.253 ± 0.02, n = 103, p = 0.7987, t test, when compared to the effects of L-AP4 on the FSK enhancement in the absence of Cd^{2+}).

Discussion

Using the sequential uptake of antibodies directed against the vesicular protein synaptotagmin I, we have found that activation of the cAMP/PKA cascade directly enhances or even causes presynaptic vesicular turnover at cerebellar granule cell synapses in culture.

Presynaptic activity has been shown to be positively modulated by cAMP increase at several synapses of the central nervous system (Chavez-Noriega and Stevens, 1992, 1994; Frey et al., 1993; Huang et al., 1994; Weisskopf et al., 1994; Salin et al., 1996; Trudeau et al., 1996; Chen and Regher, 1997; Bolshakov et al., 1997). To date, cAMP-dependent LTP has only been demonstrated at the mossy fiber–CA3 pyramidal cell synapses of the hippocampus (Weisskopf et al., 1994), in a late phase of LTP at CA3–CA1 synapses (Frey et al., 1993; Bolshakov et al., 1997), and at the parallel fiber–Purkinje cells of the cerebellum (Salin et al., 1996). Our report using cultured cerebellar granule cell synapses extends previous studies performed in cerebellar slices (Salin et al., 1996; Chen and Regher, 1997). Moreover, the high spatial resolution of the method enabled the visualization at the single-bouton level of the long-term effects of pharmacological manipulations known to cause cAMP-dependent enhancement of glutamate release. Using agents acting downstream of cAMP and at the PKA level (i.e., the cAMP analog CPT–cAMP and the PKA inhibitor Rp–cAMP), a pivotal role for PKA activation was found, in agreement with previous reports studying cAMP-dependent LTP at hippocampal synapses (Frey et al., 1993; Huang et al., 1994; Weisskopf et al., 1994; Brandon et al., 1995; Trudeau et al., 1996; Bolshakov et al., 1997).

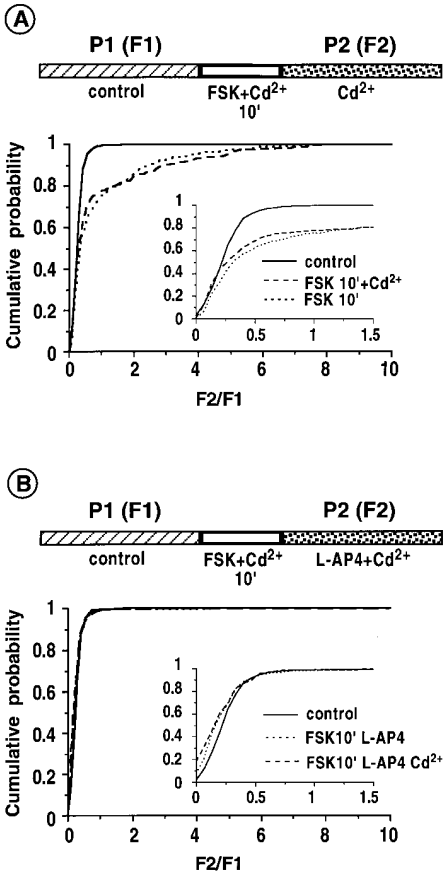

Figure 5. cAMP/PKA and mGluR Modulate Vesicular Release Downstream of Ca^{2+} Channels

Cumulative probability distributions of F2/F1 values for individual synapses showing that the long-lasting stimulating effects of (A) FSK (FSK 10′ + Cd^{2+}) and (B) the L-AP4 inhibition of the FSK-evoked vesicular cycling (FSK 10′ L-AP4 Cd^{2+}) were insensitive to 100 μM Cd^{2+}.

In addition to increased vesicular turnover at preexisting synapses, activation of the cAMP/PKA cascade caused anti–synaptotagmin I uptake at sites that were inactive during the control period, suggesting the appearance of vesicular recycling at previously silent zones. This new vesicular activity was induced by either cAMP elevation or direct PKA activation and is consistent with a presynaptic expression mechanism for cerebellar LTP (Salin et al., 1996). These data contrast with a report by Trudeau and colleagues that reported PKA increased secretory activity without changing the number of release sites (Trudeau et al., 1996). It should be noted that with FM1–43, sequestration of the indicator at existing active release sites is required prior to any manipulations. Therefore, silent synapses would not be labeled during loading of the vesicles during the control period. Another possibility is that our approach gave a "cumulative" estimation of the activity of uptake sites over a 1 hr period, whereas the FM1–43 measurements are usually done over a much shorter period (e.g., 60 s).

When boutons were classified according to their initial exocytotic activity, we found that the lower the initial

vesicular activity the higher the amount of cAMP-dependent potentiation. This finding is in agreement with several studies indicating a nonuniformal probability of release at central synapses (Rosenmund et al., 1993) and an inverse relationship between baseline release probability and the magnitude of short-term (Dobrunz and Stevens, 1997; Murthy et al., 1997) or long-term potentiation (Malgaroli et al., 1995; Ryan et al., 1996; Schultz, 1997).

Studies of both cAMP-dependent LTP at autapses of hippocampal granule cells (Tong et al., 1996) and cAMP-dependent late phase of LTP at CA3–CA1 synapses (Bolshakov et al., 1997) had led to the proposal of silent release sites that are activated upon intracellular cAMP elevation. The present results support this hypothesis. In addition to the increased vesicular cycling at existing release sites, we found that stimulation of the cAMP/PKA cascade led to the appearance of vesicular cycling at previously silent sites. Moreover, in permeabilized cells anti–synaptotagmin I labeling was observed in regions that encompass the soma and close processes, the same regions where putative "new release sites" were found in the dynamic experiments. Parallel fibers of the cerebellum are formed by axons of granule cells making glutamatergic synapses with Purkinje cell dendrites. Several lines of evidence suggest a role of the parallel fiber–Purkinje cell synapses in motor learning (Ito, 1989; Linden, 1994). Metabotropic glutamate receptors sensitive to L-AP4 (group 3 mGluRs) have been shown to be highly expressed at this synapse (Tanabe et al., 1993; Prézeau et al., 1994; Saugstad et al., 1994; Ohishi et al., 1995; Kinoshita et al., 1996), suggesting a role as glutamate autoreceptors. Knockout experiments have demonstrated that mice lacking mGluR4 (Pekhletski et al., 1996) displayed impaired cerebellar synaptic plasticity and motor performance. Thus, it was suggested that mGluR4 receptor activation tonically inhibits vesicular release, providing a presynaptic mechanism for maintaining synaptic efficacy during repetitive activation (Pekhletski et al., 1996). Because activation of L-AP4–sensitive mGluRs inhibits FSK-induced cAMP increases in brain slices and neuronal cultures (Conn and Pin, 1997), we reasoned that L-AP4 receptor activation could modulate the cAMP/PKA–dependent enhancement of vesicular release. Concentrations as low as 20 μM of L-AP4 could completely block not only the FSK-induced but also the CPT–cAMP increase of release, suggesting that L-AP4–sensitive mGluRs do not mediate their inhibitory actions via reducing the intracellular cAMP levels but rather act at a step downstream of the AC. In accord with Chen and Regehr (1997), the cAMP enhancement was independent of Ca^{2+} influx into the terminal. Similarly, L-AP4 acted downstream of Ca^{2+} influx. Interestingly, the L-AP4 inhibition was restricted to release sites active during the control period (release sites at the axon's terminal zone) and did not block the cAMP-dependent effect in regions closer to the soma. A specific localization of L-AP4 mGluRs at the site of synaptic vesicle fusion would explain this observation and support their proposed presynaptic function (Koerner and Cotman, 1981; Mayer and Westbrook, 1987; Pekhletski et al., 1996). Indeed, mGluR4a immunoreactivity has been described exclusively at presynaptic sites on cerebellar parallel fibers (Kinoshita et al., 1996). In the rat hippocampus, mGluR7 (another group 3 receptor) has also been shown to be restricted to the presynaptic grid (Shigemoto et al., 1996).

This report provides a possible mechanism underlying the cAMP-dependent presynaptic LTP of parallel fiber synapses by showing that activation of the cAMP/PKA cascade increases vesicular release at existing synapses and switches on silent release sites. Parallel fiber–Purkinje cell synapses are involved in several types of motor learning (Ito, 1989; Linden, 1994; du Lac et al., 1995); thus, it is tempting to speculate that cAMP-dependent LTP contributes to the physiological functions of these synapses.

Experimental Procedures

Cerebellar Granule Cell Culture

Primary cultures of cerebellar cells were prepared as previously described (Van-Vliet et al., 1989). Seven-day-old male mice (Iffa-Credo, Lyon, France) were decapitated, the brain was extracted, and the cerebellum was removed. After mechanical dissociation of the cerebella, cells were plated at a density of 0.5×10^6 cells/ml in 35 mm diameter Falcon tissue culture dishes precoated with 15 mg/ml poly-L-ornithine (Sigma). Cultures were kept in a humidified atmosphere of 5% CO_2/95% O_2, at 37°C, in minimal essential medium (MEM) with Earle's salts without phenol red (GIBCO, France), supplemented with glucose (33 mM), KCl (23 mM), glutamine (2 mM), 10% serum suprême (Bio Whitaker, Gagny, France), penicillin (100 IU/ml), and streptomycin (100 μg/ml). To avoid glial cell multiplication, 40 μM cytosine arabinoside was added to the medium 48 hr after plating. At the same time, half the culture medium was exchanged. Under these conditions, granule neurons represented 90% of the cells, and by 8–10 days they had developed mature synaptic contacts and could release endogenous excitatory amino acids (Van-Vliet et al., 1989).

Synaptic Uptake of Antibodies to Synaptotagmin I

Before and between antibody incubations, cerebellar granule cells were washed extensively with a serum KCl-free MEM culture medium supplemented with tetrodotoxin (5×10^{-7} M), D-APV (2.5×10^{-5} M), and kynurenic acid (2×10^{-4} M) and warmed up to 37°C in a humidified atmosphere of 5% CO_2/95% O_2. In all the experiments, anti–synaptotagmin I antibodies were added at a final dilution of 1:250 (goat) or 1:100 (rabbit) to the former medium. Cultures were incubated under a humidified atmosphere of 5% CO_2/95% O_2 during two sequential experimental epochs monitored separately by using the two different antibodies.

Indirect Immunofluorescence Detection

Cells were fixed with paraformaldehyde 4% in 120 mM glucose for 30 min at room temperature. Background noise was reduced by quenching free aldhehyde groups with 0.1 M glycine in phosphate buffered saline (Mg^{2+}- and Ca^{2+}-free, PBS, GIBCO, France), pH 7.4, for 30 min. Permeabilization was achieved with a PBS containing 0.1% Triton X-100 for 8 min. After being washed with PBS containing 20% horse serum, granule cells were incubated with the primary antibodies to β-tubulin (Sigma, 1/200) or synaptophysin (Sigma, 1/200) for 3 hr at 37°C in PBS/horse serum medium. The preparation was then washed three times for 30 min in PBS/horse serum and incubated with the secondary antibodies for 80 min at room temperature in a humidified atmosphere. For both β-tubulin and synaptophysin primary antibodies, the secondary antibody was Cy5-conjugated mouse IgG (1/200, Chemicon, Temcula, CA). The anti-goat and anti-rabbit synaptotagmin primary antibodies were revealed by Texas red–conjugated goat IgG (1/100, Jackson Immunoresearch Laboratories, West Grove, PA) and fluorescein-conjugated rabbit IgG (1/100, Chemicon), respectively. Cells were washed for 30 min with PBS/horse serum buffer, rinsed with 5 mM phosphate buffer (pH 7.4), and mounted on glass coverslips in Vectashield H-1000

(Vector Laboratories, Burlingame, CA). All experiments were made in duplicate on two to five different cultures.

Confocal Imaging

Cerebellar granule cell cultures were imaged with an Odyssey XL (Noran Instruments, Middleton, WI) laser confocal microscope equipped with an argon-krypton laser. A line of the laser beam (448, 568, and 647 nm) was selected with a band-pass filter depending on the fluorophore used, and the emitted fluorescence was collected through the appropriate barrier filter: rabbit synaptotagmin (FITC), excitation 488 nm, emission 515 nm, long-pass (LP) filter; goat synaptotagmin (Rhod), excitation 568 nm, emission 590 nm, LP filter; β-tubulin (Cy5), excitation 647 nm, emission 660 nm, LP filter.

Cells were viewed with a 63× 1.4 NA plan apochromat (Zeiss, France). The thickness of confocal images was varied by selecting different detection slits. We used a large slit (50 μm), which gave the brightest images with an accurate axial resolution of 1.3 μm. Functional synaptic boutons were first visualized as fluorescent puncta located on β-tubulin–stained neurites. Optical slices of the cells were then recorded using the normal scan mode (30 images/s with averaging 256 frames) with an image size of 320 × 240 pixels and a 400 ns dwell rate/pixel. Following capture of fluorescent images into memory of the Indy R4600SC/133 MHz Silicon Graphics station, images were processed as a t-series using the InterVision 1.4.1 software package. The boundaries of the Texas red–stained boutons were demarcated for the first image (F1), and fluorescent intensity was quantitated over the pixels within the corresponding fluorescein–stained region on the subsequent image (F2). No background subtraction was performed in order to avoid overcorrection of intensity values. The releasing activity at the single bouton level was then expressed as the F2/F1 ratio calculated using the KaleidaGraph software (USA). Statistical analyses were done with the Student's t test using Statview-Student (Abacus Concepts); $p < 0.05$ was taken as indicating statistical significance.

In order to compute and compare the behavior of a population of synapses, we plotted the F2/F1 ratio measured at individual synapses against their frequency of occurrence (frequency distribution plots; data not shown). The integral of the frequency distribution plot gave the cumulative probability plots, as shown in Figure 2C. A shift to the right indicates an augmentation of the number of synapses with high release activity.

Drugs

Drugs used were: L-AP4, tetrodotoxin, FSK, dideoxy-FSK (Sigma), Rp–cAMPs (RBI), and CPT–cAMP (Boehringer). FSK and dideoxy-FSK were made up as a 100 mM stock in ethanol and stored at −20°C. L-AP4 was made up as a 100 mM stock in 100 mM NaOH and stored at −20°C.

Acknowledgments

This research was supported by grants from the Centre National pour la Recherche Scientifique (CNRS), the European Economic Community (BIO2-CT93–0243 and BIOMED BMH4-CT95–1406), Bayer Company (Germany), Ministère de la Recherche (ACC-SV11), Région Languedoc-Roussillon, the Institut National de la Sante et de la Recherche Medicale (INSERM), the Association pour la Recherche contre le Cancer (ARC), and the Fondation pour la Recherche Medicale (FRM). The authors would like to thank Dr. A. Malgaroli for his precious help with the synaptotagmin-uptake technique and for providing the anti-synaptotagmin antibodies, Dr. G. Westbrook and Dr. J. Williams for critical reading of the manuscript, and M. Passama for the artwork.

Received September 25, 1997; revised January 30, 1998.

References

Betz, W.J., and Bewick, G.S. (1992). Optical analysis of synaptic vesicle recycling at the frog neuromuscular junction. Science *255*, 200–203.

Bolshakov, V.Y., Golan, H., Kandel, E.R., and Siegelbaum, S.A. (1997). Recruitment of new sites of synaptic transmission during the cAMP-dependent late phase of LTP at CA3–CA1 synapses in the hippocampus. Neuron *19*, 635–651.

Brandon, E.P., Zhuo, M., Huang, Y.Y., Qi, M., Gerhold, K.A., Burton, K.A., Kandel, E.R., Mcknight, G.S., and Idzerda, R.L. (1995). Hippocampal long-term depression and depotentiation are defective in mice carrying a targeted disruption of the gene encoding the RI beta subunit of cAMP-dependent protein kinase. Proc. Natl. Acad. Sci. USA *92*, 8851–8855.

Chavez-Noriega, L.E., and Stevens, C.F. (1992). Modulation of synaptic efficacy in field CA1 of the rat hippocampus by forskolin. Brain Res. *574*, 85–92.

Chavez-Noriega, L.E., and Stevens, C.F. (1994). Increased transmitter release at excitatory synapses produced by direct activation of adenylate cyclase in rat hippocampal slices. J. Neurosci. *14*, 310–317.

Chen, C., and Regher, W.G. (1997). The mechanism of cAMP-mediated enhancement at a cerebellar synapse. J. Neurosci. *17*, 8687–8694.

Conn, P.J., and Pin, J.P. (1997). Pharmacology and functions of metabotropic receptors. Annu. Rev. Pharmacol. Toxicol. *37*, 205–237.

Cotman, C.W., Flatman, J.A., Ganong, A.H., and Perkins, M.N. (1986). Effects of excitatory amino acid antagonists on evoked and spontaneous excitatory potentials in guinea-pig hippocampus. J. Physiol. (Lond.) *378*, 403–415.

Dobrunz, L.E., and Stevens, C.E. (1997). Heterogeneity of release probability, facilitation, and depletion at central synapses. Neuron *18*, 995–1008.

du Lac, S., Raymond, J.L., Sejnowski, T.J., and Lisberger, S.G. (1995). Learning and memory in the vestibulo-ocular reflex. Annu. Rev. Neurosci. *18*, 109–441.

Elferink, L.A., and Scheller, R.H. (1995). Synaptic vesicle proteins and regulated exocytosis. Prog. Brain Res. *105*, 79–85.

Elferink, L.A., Peterson, M.R., and Scheller, R.H. (1993). A role for synaptotagmin (p65) in regulated exocytosis. Cell *72*, 153–159.

Frey, U., Huang, Y.Y., and Kandel, E.R. (1993). Effects of cAMP simulate a late stage of LTP in hippocampal CA1 neurons. Science *260*, 1661–1664.

Huang, Y.Y., Li, X.C., and Kandel, E.R. (1994). cAMP contributes to mossy fiber LTP by inititating both a covalently mediated early phase and a macromolecular synthesis-dependent late phase. Cell *79*, 69–79.

Ito, M. (1989). Long-term depression. Annu. Rev. Neurosci. *12*, 85–102.

Kinoshita, A., Ohishi, H., Nomura, S., Shigemoto, R., Nakanishi, S., and Mizuno, N. (1996). Presynaptic localization of a metabotropic glutamate receptor, mGluR4a, in the cerebellar cortex: a light and electron microscope study in the rat. Neurosci. Lett. *207*, 199–202.

Koerner, J.F., and Cotman, C.W. (1981). Micromolar L-2-amino-4-phosphonobutyric acid selectively inhibits perforant path synapses from lateral entorhinal cortex. Brain Res. *216*, 192–198.

Linden, D.J. (1994). Long-term depression in the mammalian brain. Neuron *12*, 457–472.

Malgaroli, A., Ting, A.E., Wendland, B., Bergamaschi, A., Villa, A., Tsien, R.W., and Scheller, R.H. (1995). Presynaptic component of long-term potentiation visualized at individual hippocampal synapses. Science *268*, 1624–1628.

Matteoli, M., Takei, K., Perin, M.S., Sudhof, T.C., and De Camilli, P. (1992). Exo-endocytotic recycling of synaptic vesicles in developing processes of cultured hippocampal neurons. J. Cell Biol. *117*, 849–861.

Mayer, M.L., and Westbrook, G.L. (1987). The physiology of excitatory amino acids in the vertebrate central nervous system. Prog. Neurobiol. *28*, 197–276.

Murthy, V.N., Sejnowski, T.J., and Stevens, C.F. (1997). Heterogeneous release properties of individual hippocampal synapses. Neuron *18*, 599–612.

Ohishi, H., Akazawa, C., Shigemoto, R., Nakanishi, S., and Mizuno, N. (1995). Distributions of the mRNAs for L-2-amino-4-phosphonobutyrate-sensitive metabotropic glutamate receptors, mGluR4 and mGluR7, in the rat brain. J. Comp. Neurol. *360*, 555–570.

Pekhletski, R., Gerlai, R., Overstreet, L.S., Huang, X.P., Agopyan, N., Slater, N.T., Abramownewerly, W., Roder, J.C., and Hampson, D.R. (1996). Impaired cerebellar synaptic plasticity and motor performance in mice lacking the mGluR4 subtype of metabotropic glutamate receptor. J. Neurosci. *16*, 6364–6373.

Prézeau, L., Carette, J., Helpap, B., Curry, K., Pin, J.-P., and Bockaert, J. (1994). Pharmacological characterization of metabotropic glutamate receptors in several types of brain cells in primary cultures. Mol. Pharmacol. *45*, 570–577.

Rosenmund, C., Clements, J.D., and Westbrook, G.L. (1993). Nonuniform probability of glutamate release at a hippocampal synapse. Science *262*, 754–757.

Ryan, T.A., Ziv, N.E., and Smith, S.J. (1996). Potentiation of evoked vesicle turnover at individually resolved synaptic boutons. Neuron *17*, 125–134.

Salin, P.A., Malenka, R.C., and Nicoll, R.A. (1996). Cyclic AMP mediates a presynaptic form of LTP at cerebellar parallel fiber synapses. Neuron *16*, 797–803.

Saugstad, J.A., Kinzie, J.M., Mulvihill, E.R., Segerson, T.P., and Westbrook, G.L. (1994). Cloning an expression of a new member of the L-2-amino-4-phosphonobutyric acid class of metabotropic glutamate receptors. Mol. Pharmacol. *45*, 367–372.

Scanziani, M., Gahwiler, B.H., and Thompson, S.M. (1995). Presynaptic inhibition of excitatory synaptic transmission by muscarinic and metabotropic glutamate receptor activation in the hippocampus: are Ca^{2+} channels involved? Neuropharmacology *34*, 1549–1557.

Schultz, P.E. (1997). Long-term potentiation involves increases in the probability of neurotransmitter release. Proc. Natl. Acad. Sci. USA *94*, 5888–5893.

Seamon, K.B., and Daly, J.W. (1986). Forskolin: its biological and chemical properties. Adv. Cyclic Nucleotide Protein Phosphorylation Res. *20*, 1–150.

Shigemoto, R., Kulik, A., Roberts, J.D.B., Ohishi, H., Nusser, Z., Kaneko, T., and Somogyi, P. (1996). Target-cell–specific concentration of a metabotropic glutamate receptor in the presynaptic active zone. Nature *381*, 523–525.

Tanabe, Y., Nomura, A., Masu, M., Shigemoto, R., Mizuno, N., and Nakanishi, S. (1993). Signal transduction, pharmacological properties, and expression patterns of two rat metabotropic glutamate receptors, mGluR3 and mGluR4. J. Neurosci. *13*, 1372–1378.

Tong, G., Malenka, R.C., and Nicoll, R.A. (1996). Long-term potentiation in cultures of single hippocampal granule cells: a presynaptic form of plasticity. Neuron *16*, 1147–1157.

Trudeau, L.E., Emery, D.G., and Haydon, P.G. (1996). Direct modulation of the secretory machinery underlies PKA-dependent synaptic facilitation in hippocampal neurons. Neuron *17*, 789–797.

Tyler, E.C., and Lovinger, D.M. (1995). Metabotropic glutamate receptor modulation of synaptic transmission in corticostriatal cocultures: role of calcium influx. Neuropharmacology *34*, 939–952.

Van-Vliet, B.J., Sebben, M., Dumuis, A., Gabrion, J., Bockaert, J., and Pin, J.-P. (1989). Endogenous amino acid release from cultured cerebellar neuronal cells: effect of tetanus toxin on glutamate release. J. Neurochem. *52*, 1229–1239.

Weisskopf, M.G., Castillo, P.E., Zalutsky, R.A., and Nicoll, R.A. (1994). Mediation of hippocampal mossy fiber long-term potentiation by cyclic-AMP. Science *265*, 1876–1882.

Wu, L.G., and Saggau, P. (1994). Adenosine inhibits evoked synaptic transmission primarily by reducing presynaptic calcium influx in area CA1 of the hippocampus. Neuron *12*, 1139–1148.

Wu, L.G., and Saggau, P. (1995). $GABA_B$ receptor–mediated presynaptic inhibition in guinea-pig hippocampus is caused by reduction of presynaptic Ca^{2+} influx. J. Physiol. (Lond.) *485*, 649–657.

Wu, L.G., and Saggau, P. (1997). Presynaptic inhibition of elicited neurotransmitter release. Trends Neurosci. *20*, 204–212.

Zalutsky, R.A., and Nicoll, R.A. (1990). Comparison of two forms of long-term potentiation in single hippocampal neurons. Science *248*, 1619–1624.